



Development of decellularization protocols for female cat reproductive organs

Phakjira Sanguansook^a, Cristina Martínez-López^{b,c,d}, M^a. José Izquierdo-Rico^{b,c}, Carlos Martínez-Cáceres^c, Marina López-Orozco^e, Kaywalee Chatdarong^{a,**}, Francisco Alberto García-Vázquez^{c,d,*}

^a Department of Obstetrics, Gynaecology and Reproduction, Faculty of Veterinary Science, Chulalongkorn University, Bangkok, Thailand

^b Departamento de Biología Celular e Histología, Facultad de Medicina, Universidad de Murcia, Murcia, Spain

^c Instituto Murciano de Investigación Biosanitaria Pascual Parrilla (IMIB), Murcia, Spain

^d Departamento de Fisiología, Facultad de Veterinaria, Universidad de Murcia, Murcia, Spain

^e Departamento de Producción Animal, Facultad de Veterinaria, Campus de Excelencia Internacional para la Educación Superior y la Investigación "Campus Mare Nostrum", Universidad de Murcia, Murcia, Spain

ARTICLE INFO

Keywords:
Bioengineering
Decellularization
Felis catus
Scaffold

ABSTRACT

Decellularization is an innovative method to create natural scaffolds by removing all cellular materials while preserving the composition and three-dimensional ultrastructure of the extracellular matrix (ECM). The obtention of decellularized reproductive organs in cats might facilitate the development of assisted reproductive techniques not only in this species but also in other felids. The aim was to compare the efficiency of three decellularization protocols on reproductive organs (ovary, oviduct, and uterine horn) in domestic cats. The decellularization protocol involved 0.1% sodium dodecyl sulfate and 1% Triton X-100. Protocol 1 (P1) entailed 2-cycles of decellularization using these detergents. Protocol 2 (P2) was like P1 but included 3-cycles. Protocol 3 (P3) was similar to P2, with the addition of deoxyribonuclease incubation. Reproductive organs from nine cats were separated into two sides. One side served as the control (non-decellularized organ) while the contralateral side was the treated group (decellularized organ). The treated organs were subdivided into 3 groups ($n = 3$ per group) for each protocol. Both control and treated samples were analyzed for DNA content, histology (nuclear and ECM (collagen, elastin, and glycosaminoglycans (GAGs)) density), ultrastructure by electron microscopy, and cytotoxicity. The results of the study showed that P3 was the only protocol that displayed no nucleus residue and significantly reduced DNA content in decellularized samples (in all the studied organs) compared to the control ($P < 0.05$). The ECM content in the ovaries remained similar across all protocols compared with controls ($P > 0.05$). However, elastic fibers and GAGs decreased in decellularized oviducts ($P < 0.05$), while collagen levels remained unchanged ($P > 0.05$). Regarding the uterus, the ECM content decreased in decellularized uterine horns from P3 ($P < 0.05$). Electron microscopy revealed that the microarchitecture of the decellularized samples was maintained compared to controls. The decellularized tissues, upon being washed for 24 h, showed cytocompatibility following co-incubation with sperm. In conclusion, when comparing different decellularization methods, P3 proved to be the most efficient in removing nuclear material from reproductive organs compared to P1 and P2. P3 demonstrated its success in decellularizing ovarian samples by significantly decreasing DNA content while maintaining ECM components and tissue microarchitecture. However, P3 was less effective in maintaining ECM contents in decellularized oviducts and uterine horns.

1. Introduction

According to the International Union for Conservation of Nature

(IUCN) Red List, most species in the Felidae family, except the domestic cat (*Felis catus*) are considered threatened, vulnerable or endangered species (Thongphakdee et al., 2020). Therefore, the domestic cat may be

* Corresponding author at: Instituto Murciano de Investigación Biosanitaria Pascual Parrilla (IMIB), Murcia, Spain.

** Corresponding author.

E-mail addresses: kaywalee.c@chula.ac.th (K. Chatdarong), fagarcia@um.es (F.A. García-Vázquez).

<https://doi.org/10.1016/j.rvsc.2024.105257>

Received 23 November 2023; Received in revised form 27 March 2024; Accepted 8 April 2024

Available online 9 April 2024

0034-5288/© 2024 The Authors. Published by Elsevier Ltd. This is an open access article under the CC BY license (<http://creativecommons.org/licenses/by/4.0/>).

considered a valuable model for studying other species within the Felidae family or even as a model for human biomedical research, especially in the aspect of genetic disease and reproductive biology (Pelican et al., 2006; Hoenig, 2012; Jewgenow et al., 2017). Assisted reproductive techniques (ARTs) developed in domestic cats can be applied to produce offspring of other endangered feline species (Prochowska et al., 2022). Oocyte *in vitro* maturation (IVM), *in vitro* fertilization (IVF) or ovarian follicle culture are some of the ARTs studied for decades and applied in cats (Pope et al., 1997; Pope et al., 2006; Songsasen et al., 2012). However, the production and development of embryos up to the blastocyst stage still has several limitations in this species (Colombo et al., 2021). In this sense, the decellularization of tissues/organs has emerged as a novel technique for the improvement of ARTs, e.g. supporting preantral follicle growth (Alaee et al., 2021; Park et al., 2023) and increasing metaphase II (MII) development (Park et al., 2023; Fazelian-Dehkordi et al., 2022). To date, several studies have attempted to decellularize reproductive organs in different species (Alaee et al., 2021; Campo et al., 2017; Daryabari et al., 2022; Hassanpour et al., 2018; Alshaikh et al., 2020; Pors et al., 2019; Pennarossa et al., 2020; Tiemann et al., 2020; Daryabari et al., 2019; Padma et al., 2021), but not yet in felids. Decellularization is an innovative method involving the removal of cellular material from a tissue or organ while preserving its hierarchical complexity, composition, and the three-dimensional (3D) ultrastructure of the extracellular matrix (ECM) (Gilbert et al., 2006). The process of tissue/organ decellularization is generated through physical, chemical, or enzymatic processes (Kim et al., 2021). Decellularized tissue retaining intact ECM structures can facilitate the necessary interactions between cells and their surroundings, ensuring proper cell growth, differentiation, and function (Pennarossa et al., 2020). These tissues have a wide range of applications (Zhang et al., 2023), including serving as a 3D organ scaffold that provides a physical environment supporting cell growth (Kim et al., 2021; Zhang et al., 2023). Actually, successful generation of a decellularized ovarian scaffold has been generated in mouse (Daryabari et al., 2022; Alshaikh et al., 2020), rat (Alaee et al., 2021), human (Hassanpour et al., 2018; Pors et al., 2019; Mirzaei et al., 2020), and porcine (Pennarossa et al., 2020; Pennarossa et al., 2021) for further used in *in vitro* ovarian follicle culture (Alaee et al., 2021; Pors et al., 2019). After culturing preantral ovarian follicles in a decellularized ovary, the rate of antral formation, concentration of steroid hormones (estrogen and progesterone), and oocyte maturation rate were significantly higher compared to traditional two-dimensional (2D) culture (Alaee et al., 2021). In cat, techniques for *in vitro* ovarian follicle culture have been developed to access oocytes and produce embryos for offspring generation in valuable species (Jewgenow and Paris, 2006). However, the combined application of that technique with decellularized organs has not yet been explored.

The uterus is another organ that has been decellularized in several species like in porcine (Campo et al., 2017), rat (Padma et al., 2021), sheep (Tiemann et al., 2020; Daryabari et al., 2019), and human (Daryabari et al., 2022). There are two main benefits of a decellularized uterus. First, there is potential to use these decellularized tissue for transplantation, aiming to restore fertility in women and female animals with uterine factor infertility (Campo et al., 2017; Daryabari et al., 2022; Padma et al., 2021). The decellularization of donor's organ followed by recellularization with the recipient's autologous stem cells minimizes immune rejection which cause the failure of transplantation (Campo et al., 2017). Second, decellularized uterine tissue can be employed to generate hydrogels from ECM for used as biocompatible tissue-specific substrates for cell and embryo culture (Campo et al., 2019a; López-Martínez et al., 2021). In this context, ECM hydrogels obtained from porcine decellularized uterus combined with growth factors, have been used to regenerate endometrial tissue and restore fertility in mice with endometrium pathologies (López-Martínez et al., 2021). Moreover, there have been attempts to generate hydrogel using decellularized rabbit oviduct. This hydrogel, designed to mimic the native oviductal

environment, was used to culture two-cell rabbit embryos. Metabolomic analysis revealed that this hydrogel may include signaling molecules and release compounds beneficial for embryo metabolism (Francés-Herrero et al., 2021).

The benefits of decellularized reproductive tissue mentioned above raise interest in adapting this method to use with domestic cats as well. *In vitro* embryo production technique in domestic cats still required further development (Colombo et al., 2021). Both the 3D decellularized scaffold and tissue-specific hydrogel will facilitate the development of ARTs in felids. Thus, the initial step involves performing with decellularization in the cat's reproductive tract before implementing more advanced techniques. Then, the objective of this research is to, for the first time, conduct decellularization of female reproductive organs of domestic cats, including the ovary, oviduct, and uterine horn by comparing the efficiency of three different protocols. The success of each protocol was evaluated by comparing DNA quantification, histology analysis (which included evaluation of nuclear density and ECM components), and ultrastructure analysis (including scanning and transmission electron microscopy) between decellularized and native (non-decellularized) organs. Additionally, cytotoxicity of decellularized tissues was assessed through their interaction with sperm.

2. Material and methods

2.1. Animals and reproductive organs

Nine female domestic cats ($n = 9$) aged between 6 and 9 months were included in this study. Reproductive organs, including ovaries, oviducts, and uterine horns were collected after ovariohysterectomy at local veterinary clinics. The organs were transported on ice to the laboratory and frozen at -20°C until use. Given that this project used reproductive organs from pet cats (regularly spayed at local veterinary clinics) which were animal remains awaiting disposal, ethical approval was not required from the institution.

2.2. Experimental design

A scheme showing the overall experimental design is presented in Fig. 1. After thawing the organs at room temperature, the reproductive tracts from each cat were separated into two sides (one side was the control (non-decellularized organs including ovary, oviduct, and uterine horn), while another side was the treatment (decellularized organs)). The treatment group was further divided into 3 groups ($n = 3$ reproductive tracts per each group) for the application of Protocol 1, Protocol 2 or Protocol 3 (Table 1). Before and after decellularization process, each reproductive tract was photographed and weighed by a precision digital scale (BH600, Gram Precision, Barcelona, Spain). Then, the reproductive tract was dissected into the ovary, oviduct, and uterine horn. Both control and decellularized samples were then subdivided into five parts, enabling analysis of DNA content, histology analysis, scanning electron microscopy, transmission electron microscopy, and cytotoxicity assessment.

2.3. Decellularization of organs

After washing the organs for 1 h in phosphate buffered saline solution (PBS), decellularization was performed using three different protocols (Table 1). Protocol 1 consists of two cycles (each lasting 24 h), based on previous literature (Campo et al., 2017). Briefly, one cycle involved the immersion of the reproductive tracts in 0.1% Sodium dodecyl sulfate (SDS, Sigma Aldrich, St. Louis, USA) for 18 h, followed by distilled water for 30 min, 1% Triton X-100 (Sigma Aldrich, St. Louis, USA) for 30 min, and PBS for 5 h. Then, this cycle was repeated for other 24 h. All steps were carried out using an orbital shaker (Vibrax VXR shaker, IKA, Germany) at 150 rpm at 4°C . Protocol 2 was similar to Protocol 1, but the samples in this protocol underwent three cycles

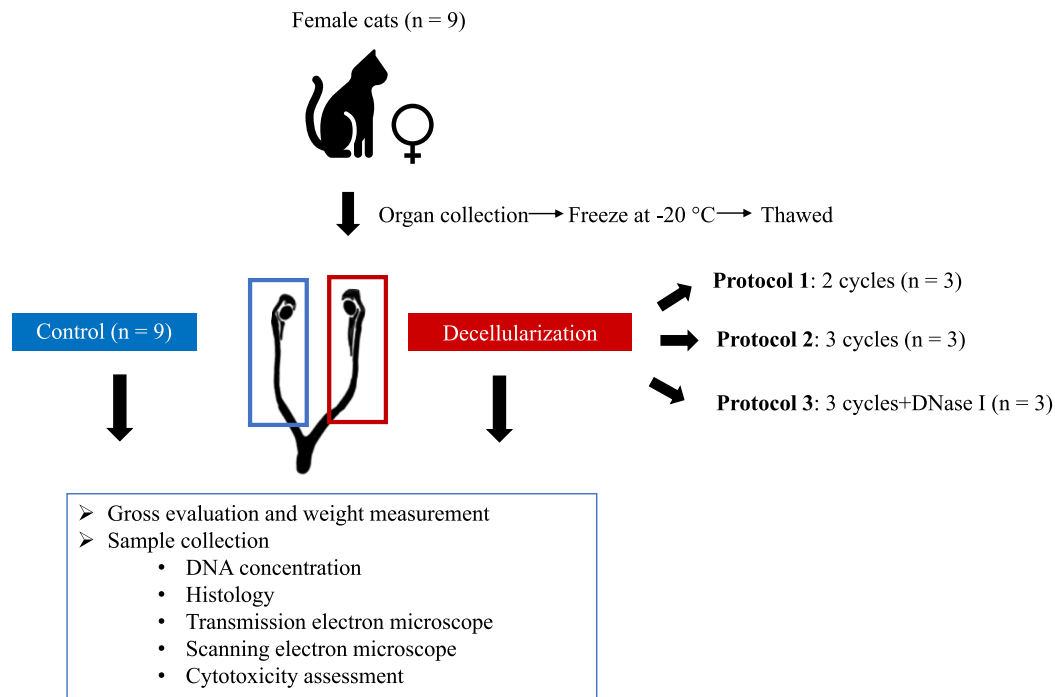


Fig. 1. Schematic representation of the experimental design followed in the study. Each side of the reproductive tracts was separated into controls and treatments (decellularized samples). The decellularized samples were further subdivided into 3 groups ($n = 3$ reproductive tracts per group) for entering Protocol 1, Protocol 2, or Protocol 3. Thereafter, both control and decellularized samples underwent gross evaluation and weight measurement. Then, each sample was dissected into ovary, oviduct, and uterine horn. Each organ was then evaluated for DNA concentration, histology, ultrastructure (using transmission and scanning electron microscope), and cytotoxicity assessment.

instead of two (as in the Protocol 1). In Protocol 3, the samples were entered the same three cycles, but additionally incubated for 24 h at 37 °C in deoxyribonuclease (DNase I) (Cat. N°. 04716728001, Sigma-Aldrich, Spain) diluted to a concentration of 100 U/mL according to manufacturer's protocol. The samples were then washed with PBS three times for 30 min each. During DNase I incubation, each sample was placed in a tube containing 5 mL of DNase I solution. The reagents were freshly prepared before each incubation, with 1 L of these reagents poured into a plastic box that used for incubated samples.

2.4. DNA quantification

At least 5 mg of tissues were kept at -20 °C for further DNA measurement. The DNA quantification assay was performed using Gentra Puregene tissue kit (Qiagen, Hilden, Germany) according to the manufacturer's protocol. DNA yield was measured by NanoDrop™ 2000/2000c Spectrophotometer (ThermoFisher scientific, Massachusetts, USA). Due to concerns about how changes in final weight might affect DNA concentration, normalization to the initial wet weight was calculated using the formula described in previous literature (Bruyneel and Carr, 2017).

2.5. Histological analysis

The ovary, oviduct, and uterine horn samples were fixed in 4% paraformaldehyde overnight at room temperature, followed by storage at 4 °C in 70% ethanol until further processing and paraffin-embedding. The tissues were sectioned in 4 µm-thick slices and stained with a standard Hematoxylin and Eosin (H&E) procedure to evaluate the nuclear density. Commercial kits for Masson's Trichrome (with aniline blue) (BioOptica, Milano, Italy), Orcein (BioOptica, Milano, Italy), and Alcian blue (Vector Laboratories, Burlingame, USA) stains were used to evaluate the main components of ECM (collagen, elastic fibers, and GAGs respectively). All stained sections were digitalized by using a

brightfield high-resolution digital slide scanner system (Pannoramic Midi II (3D Hitech, Budapest, Hungary)), and examined with a specialized software (SlideViewer, ver. 2.6.0.166179, 3D Hitech). Representative images from all sections were then obtained in ten high-power fields (HPF) (X 400) for nuclear determinations and a minimum of 6 medium-power fields (MPF) (X 200) for ECM component investigations, and digital analysis was finally performed by using a freeware software (Image J, Ver. 2.9.0, National Institutes of Health, Bethesda, Maryland, USA). To nuclear determination, a direct counting systematic method was followed to determine the number of viable nuclei in all HPF. To analyze ECM density, each representative image was color deconvoluted with a specialized plug-in appropriate for the stain employed. The measurement of each component (collagen, elastic fibers, and GAGs) was determined by using the appropriate color deconvoluted channel and calculating the percentage (%) of distribution of such component within the representative image. Additionally, to simultaneously examine the presence of nuclear remnants within the tissues, a fluorescent DAPI (4',6-diamidino-2-phenylindole) assay was conducted on paraffin-embedded sections. The samples were incubated in DAPI (diluted at 1:1000, Ref. 62,248, Thermo Scientific, Rockford, Illinois, USA) for 15 min at room temperature. Subsequently, the DAPI-stained sections were observed using fluorescence microscopy equipped with the SR LED-DA ZERO FL FILTER, employing an excitation wavelength of 378 nm and an emission wavelength of 432 nm, with respective bandwidths of 50 nm and 36 nm.

2.6. Scanning and transmission electron microscopy

Representative samples were fixed in McDowell solution (containing 1% glutaraldehyde, 4% formaldehyde, and 0.1 M cacodylate buffer) 4 °C overnight. Then, they were immersed in a washing solution (cacodylate buffer containing 8% saccharose) and stored at 4 °C until further processing. For scanning electron microscopy, the samples were post-fixed in 1% osmium tetroxide at 4 °C for 1 h, followed by immersion in a

Table 1
Decellularization protocols used for female reproductive organs in the domestic cat (*Felis catus*).

Protocol 1: Two cycles			
Step	Reagent	Duration	
Cycle 1	0.1% SDS	18 h	
	Distilled water	30 min	
	1% Triton X-100	30 min	
Cycle 2	PBS	5 h	
	0.1% SDS	18 h	
	Distilled water	30 min	
	1% Triton X-100	30 min	
	PBS	5 h	
	Protocol 2: Three cycles		
Step	Reagent	Duration	
Cycle 1	0.1%SDS	18 h	
	Distilled water	30 min	
	1% Triton X-100	30 min	
Cycle 2	PBS	5 h	
	0.1%SDS	18 h	
	Distilled water	30 min	
	1% Triton X-100	30 min	
	PBS	5 h	
	Cycle 3	0.1%SDS	18 h
Distilled water		30 min	
1% Triton X-100		30 min	
	PBS	5 h	
	Protocol 3: Three cycles + DNase I		
	Step	Reagent	Duration
Cycle 1	0.1%SDS	18 h	
	Distilled water	30 min	
	1% Triton X-100	30 min	
Cycle 2	PBS	5 h	
	0.1%SDS	18 h	
	Distilled water	30 min	
	1% Triton X-100	30 min	
	PBS	5 h	
	Cycle 3	0.1%SDS	18 h
Distilled water		30 min	
1% Triton X-100		30 min	
	PBS	5 h	
	DNase I	24 h	
	PBS	30 min × 3 times	

washing solution overnight. Next, they were dehydrated through a graded series of acetone and coated with a 5 nm layer platinum. The samples were then observed using a field emission scanning electron microscopy (FE-SEM) model Apreo S (thermo scientific, USA) at 5 kV, 0.3 nA, and a working distance of 10 mm. For transmission electron microscopy, the samples were post-fixed in 1% osmium tetroxide at 4 °C for 2 h 30 min, put in washing solution for 12 h, stained in uranyl acetate at 4 °C for 2 h, and then dehydrated through a graded series of alcohol and incubated in 100% propylene oxide for 15 min twice. Resin was used to make samples into blocks, which were then cut using an ultramicrotome. The sections were coated with uranyl acetate and lead citrate before observation using a transmission electron microscopy (JEM-1011, JEOL, Japan).

2.7. Evaluation of scaffold cytotoxicity

To assess the cytotoxicity of decellularized tissue, a sperm-scaffold interaction study was conducted. This study was carried out with decellularized tissue obtained from Protocol 2 and Protocol 3. In both cases, cytotoxicity was evaluated after completing the corresponding decellularization protocol and after 24 h of additionally washing the tissue with PBS. Therefore, for each protocol and tissue, three experimental groups were established: Control (semen sample), tissue_0h (semen sample with decellularized tissue without additional washes), and tissue_24h (semen sample with decellularized tissue additionally washed for 24 h). Prior to the incubation with sperm, the tissues were weighed, and a sample size of 8.8 ± 1.68 mg (mean \pm SD) was

determined to minimize study variability due to weight differences. The incubation method used porcine sperm because it is easy to collect, of high quality and motility, and shows uniform standards across different ejaculates, due to thorough selection of boars. The rich fraction of ejaculates from Pietrain boars, were collected at Spermatica Reproduction S.L. (Lorca, Spain) by using the gloved hand technique after a 3–5 days of abstention. In the laboratory, semen from five males was pooled. One mL of this pooled semen was allocated to each experimental group, followed by the addition of the tissue sample. The samples were then incubated for 1 h at 38.5 °C in a thermoblock (AccuBlock™ Digital Dry Bath, Labnet International). Post-incubation, sperm parameters including sperm motility, viability, and mitochondrial activity were assessed. Motility was evaluated using Computer-Assisted Semen Analysis (CASA) with the ISAS® software (PROiSER R + D S.L., Valencia, Spain), coupled with phase contrast microscopy (10× negative phase contrast objective; Leica DMR, Wetzlar, Germany) and a digital camera (Basler Vision, Ahrensburg, Germany). Viability was determined using the propidium iodide (PI) fluorochrome (P-4170 Sigma-Aldrich, Madrid, Spain). Sperm mitochondrial activity was assessed using the JC-1 fluorochrome (5,5',6,6'-tetrachloro-1,1',3,3'-tetraethylbenzimidazolylcarbocyanine iodide; ThermoFisher Scientific Inc., MA, USA). The samples were evaluated using a fluorescence microscope (Leica® DM4000 Led, Wetzlar, Germany, 495/520 nm).

2.8. Statistical analysis

Weight, DNA quantification, and number of nuclei were expressed as mean \pm SD. Sperm parameters, percentage of collagen, elastic fibers, and GAGs were expressed as mean \pm SEM (standard error of the mean). All statistical analysis was performed using Graphpad prism 9 (Graph-Pad Software, San Diego, CA, USA). All data were first tested for normality using Shapiro-Wilk test. Weight data were compared using ANOVA with Tukey's multiple comparisons test. DNA content, histological data, and sperm parameters were compared using Kruskal-Wallis test with pairwise comparison or ANOVA with Tukey's multiple comparisons test depending on normality test. For each sperm parameter, a comparison was made among the three experimental groups within each protocol (Control, tissue_0h, and tissue_24h), while all remaining data were compared between each protocol (Protocol 1, Protocol 2, and Protocol 3). Statistical significance was considered when the *p*-value was lesser than 0.05.

3. Results

3.1. Gross morphology of the genital tract

After each decellularization protocol, the color of the reproductive tract, including ovary, oviduct, and uterine horn, changed from pink to white. However, the samples retained their gross appearance without any deformation in all protocols used (Fig. 2A). The weight of reproductive tract significantly increased in Protocol 2 ($P < 0.05$) while Protocol 1 and Protocol 3 showed not significant differences with controls ($P > 0.05$) (Fig. 2B).

3.2. Nucleus counting and DNA quantification

H&E staining revealed significant reductions in visible nuclei in every decellularized organ for all tested protocols compared to the controls (Fig. 3A-F) ($P < 0.05$). However, decellularized tissues from Protocol 1 and Protocol 2 still had some nucleus debris and a more basophilic background, whereas decellularized tissues from Protocol 3 displayed no nucleus residue (Fig. 3A-C and supplementary fig. S1). The successful removal of cellular material was confirmed through DNA quantification. DNA concentration between the control group and samples after undergoing Protocol 1 and Protocol 2 showed no significant differences ($P > 0.05$) in each evaluated organ. However, there

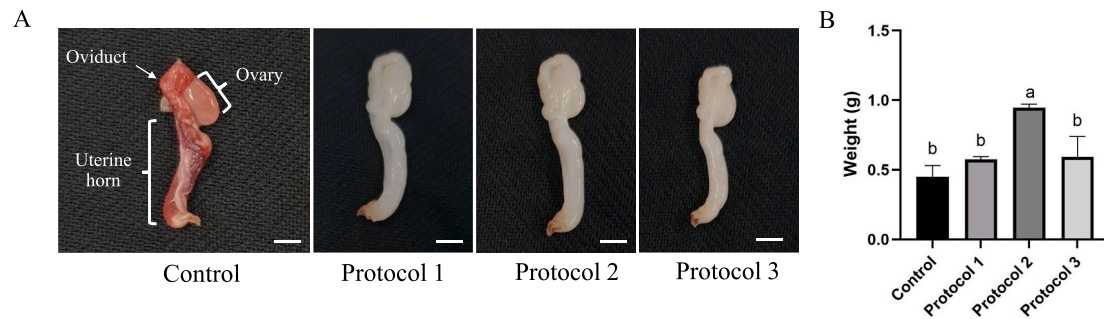


Fig. 2. Visual and macroscopic findings of cat reproductive organs subjected to decellularization protocols. (A) Macroscopic inspection of the control reproductive tract and samples after entered to each decellularization protocol. Scale bars = 5 mm. (B) The weights of reproductive tracts were measured and compared between the control (native organs without any treatment) and sample after undergoing each decellularization protocol. Different letters (a, b) on the bars indicate significant differences ($P < 0.05$). Data are expressed as mean \pm SD.

were significant reductions in DNA content ($P < 0.05$) in samples after entering Protocol 3 when compared with the controls (Fig. 3G-I). The existence of DNA was verified through DAPI staining (Supplementary Fig. S2), indicating the absence of DNA in decellularized tissues from Protocol 3. Additionally, scatter plot indicating individual value of DNA concentration was demonstrated in supplementary fig. S3. Cross-sectional histological micrographs were shown in supplementary fig. S4. In general, no thickness-associated inefficiencies or edema were observed.

3.3. ECM evaluations

Decellularized ovaries from every protocol showed no significant difference in all ECM content when compared with the control group ($P > 0.05$) (Fig. 4A,D,G,J). Regarding oviducts, all decellularization protocols resulted in similar levels of collagen when compared to the control (Fig. 4E). While decellularized oviducts from Protocol 1 and Protocol 2 had constant level of elastic fibers and GAGs compared to control, those from Protocol 3 demonstrated significant decreased in elastic fibers and GAGs ($P < 0.05$) (Fig. 4H,K). In the case of uterine horns, Protocols 1 and 2 showed no significant differences in all ECM content compared to the control group. However, decellularized uterine horns from Protocol 3 demonstrated significant decreased in all ECM contents when compared with the control group ($P < 0.05$) (Fig. 4F,I,L).

3.4. Ultrastructure analysis

Scanning electron microscopy revealed that the microarchitecture of the decellularized sample was maintained when compared with the control group (Fig. 5 and supplementary fig. S5). Cross-sections of decellularized ovary displayed a complex collagen fiber network, and porous scaffolds that used to be occupied by different cell types were even observed. The outer and inner surfaces of organs maintained their structure. The outer surface of the oviduct showed smooth serosa in both the control (Fig. 5B) and decellularized samples (Fig. 5E). Similarly, the inner (luminal) side of uterine horn showed structure of uterine glands in both the control (Fig. 5C) and decellularized samples (Fig. 5F). In transmission electron microscopy, while several nuclei were found in the control samples, no nuclear debris were observed in decellularized samples. Although the structure of the residual collagen fibers was preserved, a reduction in fiber density was observed in decellularized uterine horn (Fig. 6).

3.5. Cytotoxicity assessment

Result of cytotoxicity evaluation using sperm-scaffold interaction was shown in Fig. 7. Viability and mitochondrial activity of sperm that incubated with decellularized tissue without additional washes

(tissue_0h) decreased when compared to control ($P < 0.05$), however viability and mitochondrial activity of sperm that incubated with decellularized tissue additionally washed for 24 h (tissue_24h) were not significant different from control ($P > 0.05$). Total motility also demonstrated the same trend except in sperm that were incubated with decellularized ovary and uterine horn from Protocol 3 which showed a reduction of total motility in both tissue_0h and tissue_24h ($P < 0.05$). In addition, the reduction of progressive motility was observed in sperm which incubated with decellularized tissues without additional washes (tissue_0h) and decellularized oviduct and uterine horn from Protocol 3 additionally washed for 24 h (tissue_24h) ($P < 0.05$).

4. Discussion

Decellularization of reproductive organs can further facilitate the development of ARTs including *in vitro* follicle development and oocyte maturation. (Francés-Herrero et al., 2023). Given that studies have shown that ARTs techniques developed in domestic cats can benefit not only wild felid species (Tipkantha et al., 2016; Zahmel et al., 2022), but also humans (Comizzoli et al., 2018), it is worth optimizing the protocol for decellularize cat's reproductive organ. In this study, three decellularization protocols were used, among which only Protocol 3 successfully removed all cellular materials from cat's ovary, oviduct, and uterine horn. The reproductive tract of female cats serves as a suitable model for optimizing protocols and further transforming them into products (e.g. ECM scaffold, ECM hydrogel). It shares some of reproductive characteristics similar to humans and has a comparable oocyte structure (Wildt et al., 2010). Moreover, cat's reproductive tracts are easy to acquire without the need to sacrifice the animal. The whole ovary, oviduct, and some parts of uterus remains as disposal products after routine spaying of female cats. More than forty thousand of these operations are performed every year across the United States and Canada (McIntyre et al., 2010). The research here represents the first attempt to decellularize domestic cat's reproductive organs. Since no protocol had been developed for cats yet, we initially used a decellularization protocol (Protocol 1) adapted from porcine species (Campo et al., 2017). This protocol involved incubating samples in ionic detergent (SDS) and non-ionic detergent (Triton X-100) for two cycles. Additionally, we developed our own protocol (Protocol 2) by adding an extra cycle of detergents and combining it with the enzymatic method (Protocol 3). Although the original protocol used whole organ perfusion technique to expose the tissue to these detergents (Campo et al., 2017), our study employed an agitation and immersion method to allow the solution to permeate through the tissue and facilitate the removal of cellular material (Gilbert et al., 2006). SDS acts as a cell membrane solubilizing agent, while Triton X-100 gently removed cells by disrupting lipid-lipid and lipid-protein interactions (Gilbert et al., 2006; Neishabouri et al., 2022; Hrebikova et al., 2015). All protocol also

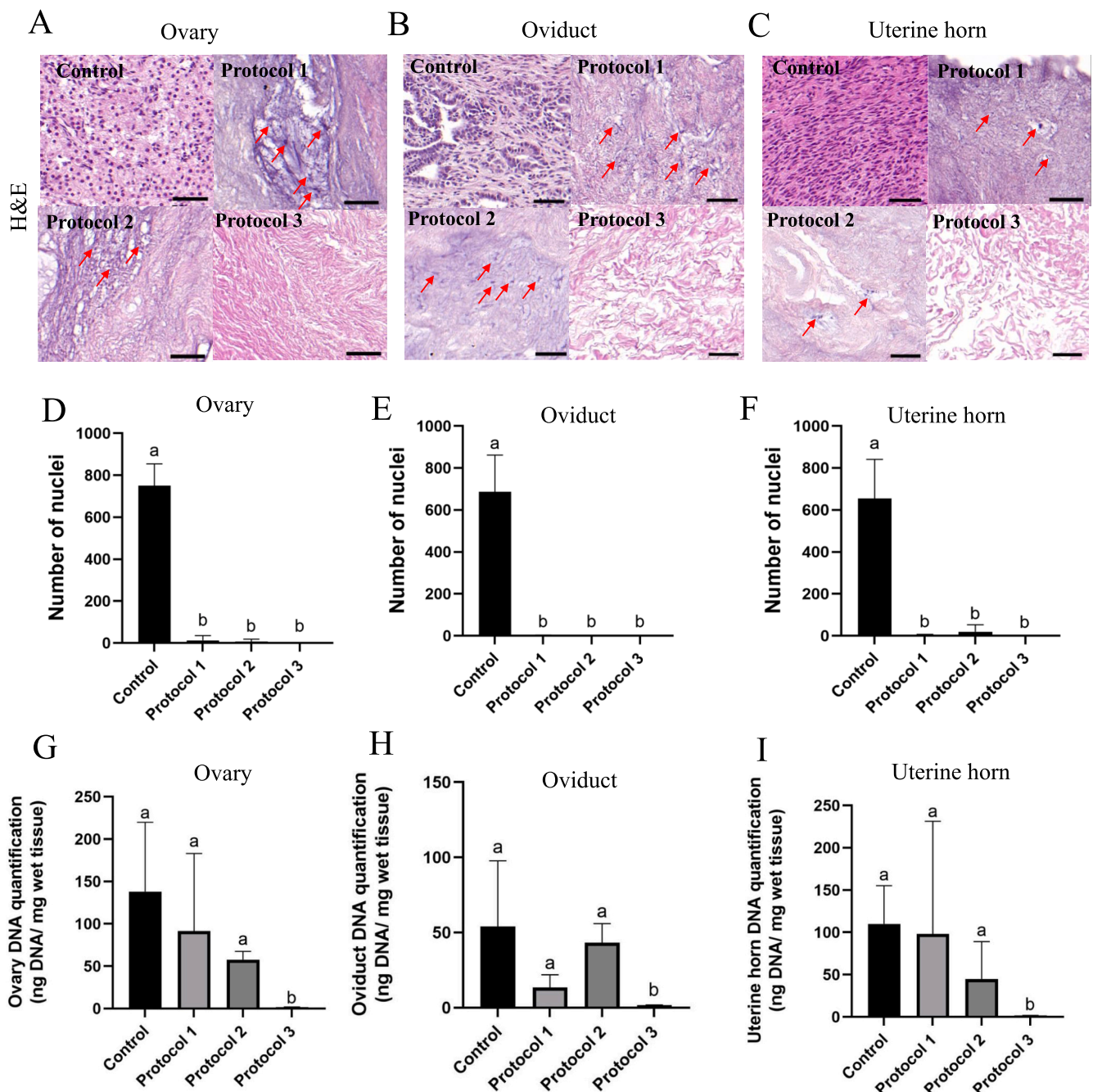


Fig. 3. (A-C) Histological micrographs of control (native tissues) and decellularized ovary, oviduct, and uterine horn from each protocol are shown. Number of nuclei comparison by hematoxylin and eosin (H&E) staining after decellularization protocols in the cat ovary (A,D), oviduct (B,E), and uterine horn (C,F). The red arrow in the image indicates nucleus debris. Visible nuclei were counted in ten random high-power fields (400×) in each organ. Scale bars = 50 μm. (G-I) Bar-graphs showing DNA quantification of the ovary (G), oviduct (H), and uterine horn (I) for the three protocols used in the study. Data are expressed as mean ± SD. Different letters (a, b) on the bars indicate significant differences ($P < 0.05$). (For interpretation of the references to color in this figure legend, the reader is referred to the web version of this article.)

included the freeze-thaw process, forming intracellular crystals that led to cell lysis (Neishabouri et al., 2022). This freeze-thawed process was reported to increase the efficiency of uterine decellularization protocol (Masoomikarimi et al., 2023).

After decellularization, gross morphology inspection is the initial assessment step to determine the transparency level of decellularized tissue compared to native tissue (Neishabouri et al., 2022). Normally, the change from the pink color of the original tissue to opaque white often suggests a significant reduction in cellular components (Hassanpour et al., 2018; Pennarossa et al., 2020); however, further accurate

assessments are essential to determine the success of decellularization (Neishabouri et al., 2022; Crapo et al., 2011). Although only decellularized organs from Protocol 2 showed significant alteration in weight, it is a trend that the weight of decellularized tissue from every protocol increased. Theoretically, weight should decrease after decellularization because some cell materials are removed. However, our result came out in a contradictory way, suggesting that some foreign factors might have caused this weight gain. A previous study suggested that it might be water that replaced cellular materials, since the wet-to-dry ratio increases after decellularization (Bruyneel and Carr, 2017). It was

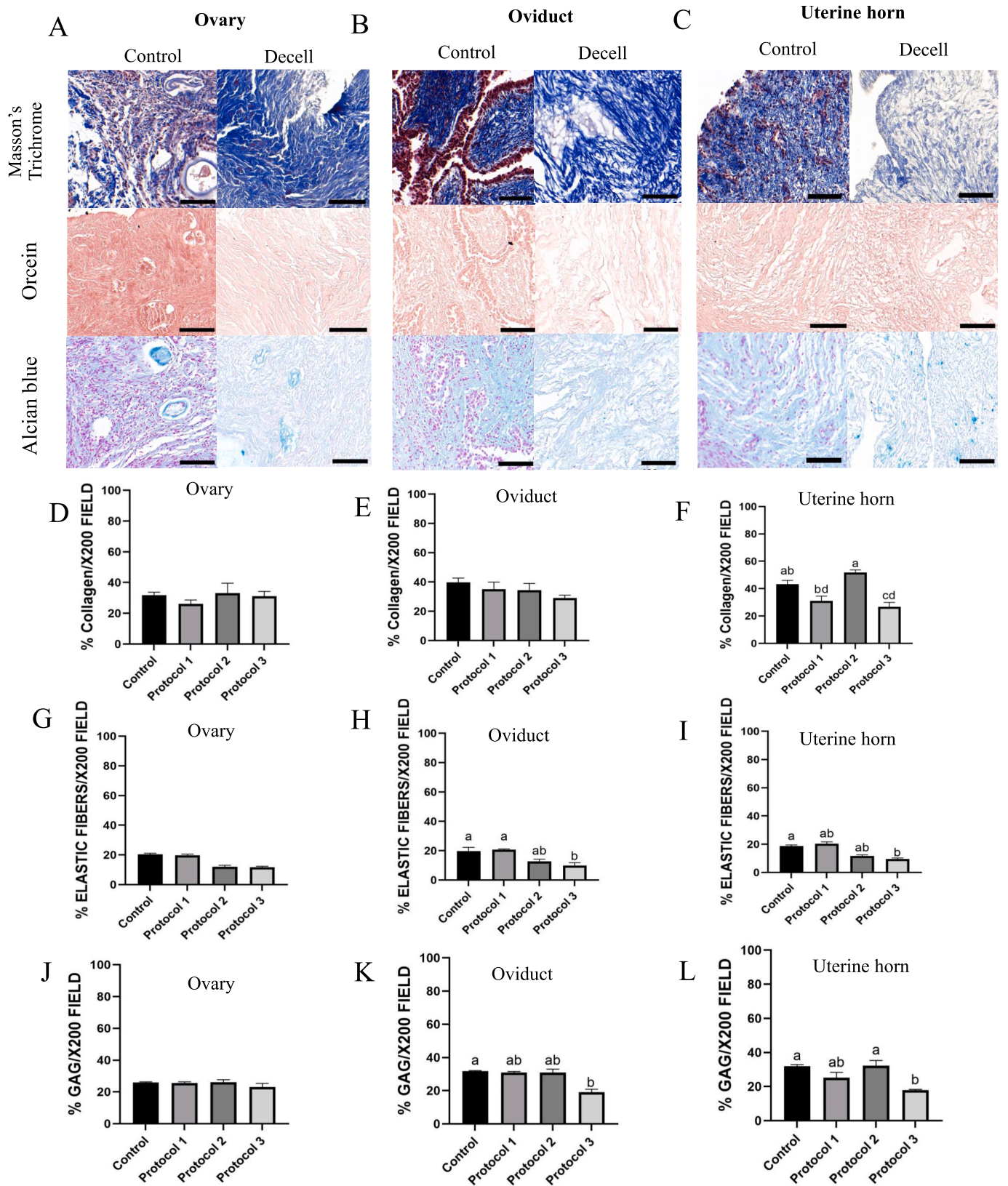


Fig. 4. Extracellular matrix (ECM) structure assessment comparing control and decellularization protocols. Histological slides of the ovary (A,D,G,J), oviduct (B,E,H,K), and uterine horn (C,F,I,L) are shown. Masson's trichrome staining, Orcein staining, and Alcain staining were performed to evaluate collagen (%), elastic fibers (%), and GAGs (%) respectively. Control refers to native organs while Decell refers to decellularized samples (Protocol 3). Scale bars = 100 μ m. Data are expressed as mean \pm SEM. Different letters (a,b,c,d) on the bars indicate significant differences ($P < 0.05$).

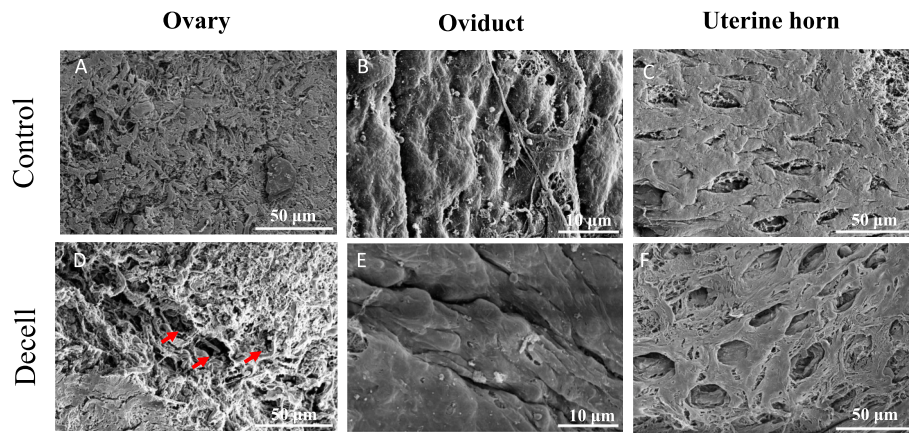


Fig. 5. Scanning electron microscopy comparison of control samples (A–C) and decellularized samples (D–F) from Protocol 3. The internal part of control ovary (A) and decellularized ovary (D) are shown. Porous structures once filled by different cell types are indicated by red arrows. Both control (B) and decellularized (E) oviducts have a smooth surface serosa. The structure of uterine glands was observed in both control (C), and decellularized (F) uterine horn. Ovary and uterine horn are at x 700 magnification, scale bars: 50 µm, while oviduct is at x 2800 magnification, scale bars: 10 µm. (For interpretation of the references to color in this figure legend, the reader is referred to the web version of this article.)

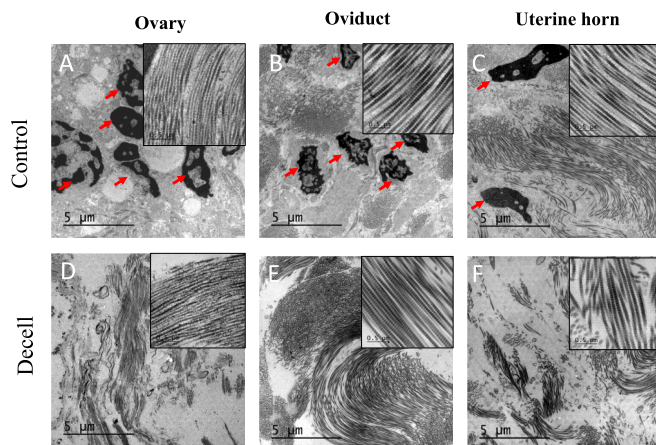


Fig. 6. Transmission electron microscopy comparison of control samples (A–C) and decellularized samples (D–F) from Protocol 3. Ovary (A,D), oviduct (B,E), and uterine horn (C,F) were separately observed (x 6000 magnification, scale bars: 5 µm). The red arrows indicate the nucleus presented only in controls. The amplification pictures show the arrangement of collagen fibers which were demonstrated in both control and decellularized samples (x 40,000 magnification, scale bars: 0.5 µm). (For interpretation of the references to color in this figure legend, the reader is referred to the web version of this article.)

hypothesized that the weight gain that occurred in this study might come from water or other remaining substances (e.g., SDS or PBS) that replace cellular materials. This weight gain has been considered a factor that may interfere with DNA concentration (the total DNA/mg of ECM), so the formula for normalization to the initial wet weight was used in this study (Bruyneel and Carr, 2017). Nonetheless, it is still debatable whether wet-ECM weight or dry-ECM weight should be used for normalization, as the measured dsDNA concentration depends on the ECM state used to extract DNA (Dhandapani and Vermette, 2023). Our study, along with other recent studies in the reproductive field, used wet-ECM as a reference when calculating DNA concentration (Campo et al., 2017; Pennarossa et al., 2020; Almeida et al., 2023). However, perhaps further studies on the effect of ECM state and ECM weight on quantitative values (e.g., DNA content) should be performed.

To assess the success of each decellularization protocol, we followed the criteria which stated that a decellularized ECM should have <50 ng DNA per mg ECM weight and lack of visible nuclear material in tissues sections evaluated with H&E (Crapo et al., 2011). When comparing the

different decellularization methods, Protocol 3 was more efficient than Protocols 1 and 2 as it significantly reduced DNA content in decellularized samples compared to the controls. Protocol 3 was considered the only successful method because its decellularized samples passed the defined cut-off value for DNA quantification (<50 ng per mg tissue) and exhibited no remnants of nuclear material. This result is in accordance with previous literature, which mentioned that a decellularization protocol that combines physical, chemical, and enzymatic methods is considered as the most effective and robust (Gilbert et al., 2006; Grauss et al., 2003). Our result aligns with a previous study indicating that incubation of tissue in detergent alone demonstrated remnants of basophilic nuclear residues, but complete loss of cellular materials occurred after DNase addition (Grauss et al., 2003). Furthermore, Protocol 3 effectively maintained ovarian ECM contents and tissue microarchitecture, as demonstrated in both scanning and transmission electron microscopy.

The cytotoxicity of decellularized tissues was assessed through their interaction with sperm that are the representative cells naturally found in reproductive tract. Sperm cells are highly sensitive to changes in their environment and to toxins, including detergents (Dietrich et al., 2007), making them ideal indicators of cytotoxicity. If a scaffold contains detergents or other cytotoxic substances, it could result in sperm mortality or functional impairment. Our cytotoxicity results confirm the safeness of decellularized tissues additionally washed for 24 h (tissue_{24h}), as sperm cells that interacted with these samples maintained their viability and demonstrated almost no functional impairment compared to the control. It is crucial to have sufficient additional wash after the decellularization process to remove detergents, and other residues that could potentially be harmful or have toxic influence on reseeding cells (Gilbert et al., 2006; Cebotari et al., 2010).

Our success in decellularizing the ovary holds great promise for future application in the future such as creating an ovarian scaffold for follicle culture (Nikniaz et al., 2021), an ECM-based artificial ovary (Wu et al., 2023), or an ECM-based hydrogel for follicle culture (Francés-Herrero et al., 2023). The ECM plays a crucial role in folliculogenesis by providing structural support and a platform for cell differentiation, proliferation, and steroidogenesis (Woodruff and Shea, 2007). Additionally, the ECM sequesters paracrine regulatory factors involved in folliculogenesis (Alaee et al., 2021). The decellularized ECM generated from cat ovaries will facilitate the development of a suitable system for feline follicle culture, which may be benefit for ARTs in domestic cat and endangered felid species. Regarding to oviduct and uterine horn, Protocol 3 led to a significant decrease in DNA content and nuclei, demonstrating the success of the decellularization process. However,

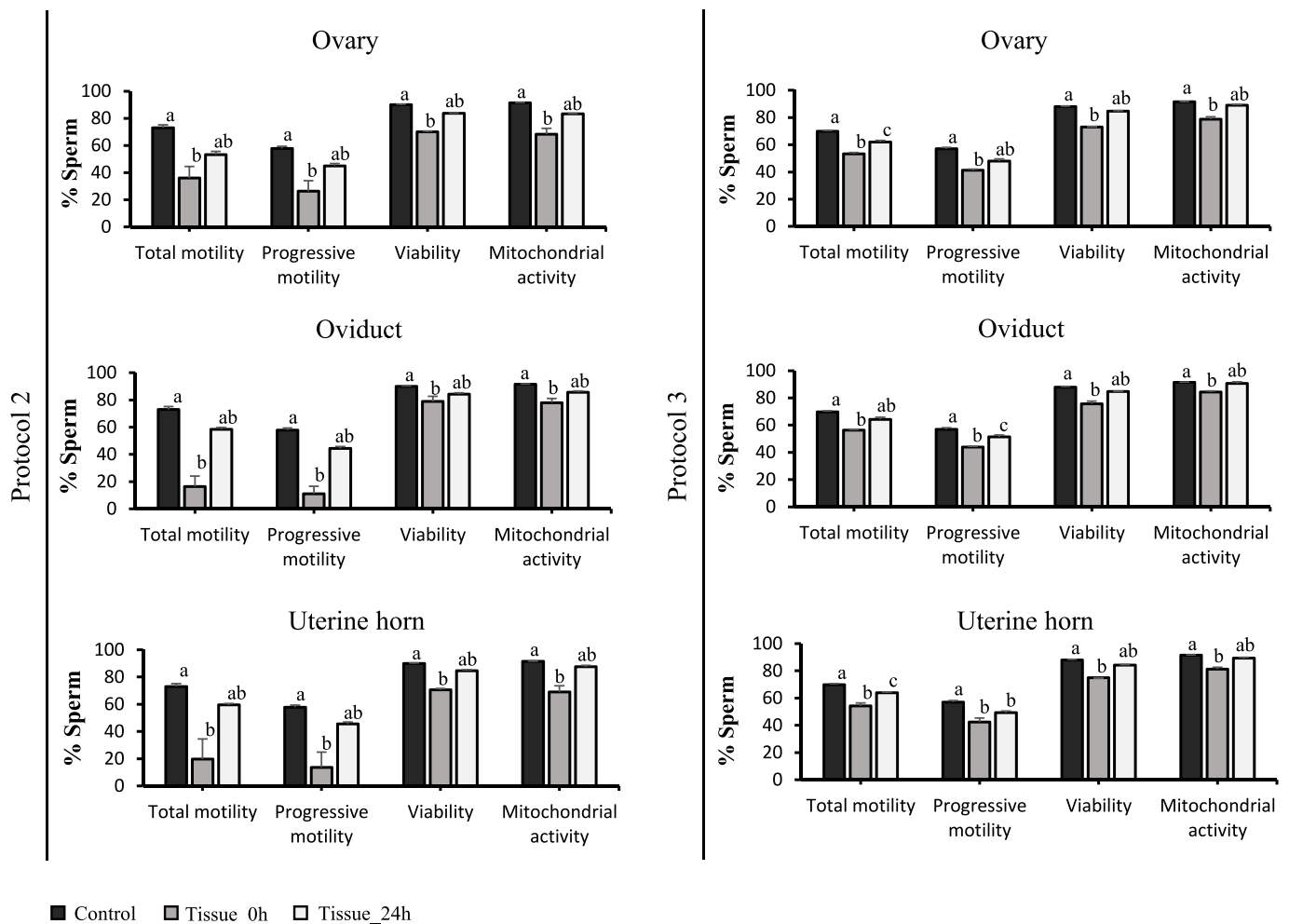


Fig. 7. Cytotoxicity assessment of decellularized tissue from Protocol 2 and Protocol 3 by sperm-scaffold interaction. Sperm parameters including total motility, progressive motility, viability, and mitochondrial activity are expressed as mean ± SEM. A comparison was made among the three experimental groups (Control, tissue_0h, and tissue_24h) within different organs from each protocol. Different letters (a,b,c) on the bars indicate significant differences (P < 0.05).

there was a significant reduction in elastic fibers and GAGs in the decellularized oviduct, and all evaluated ECM components significantly decreased in the decellularized uterine horns from Protocol 3. Previous uterus and oviduct decellularization protocol that used combination of enzymatic treatment with DNase also demonstrated a reduction in ECM contents in decellularized samples, especially a significant decrease in GAGs (Tiemann et al., 2020; Francés-Herrero et al., 2021). Hence, these protocols will require further optimization. Factors such as detergent type, exposure time, and incubation temperature contribute to different results in decellularization. Therefore, it is necessary to balance these factors to sufficiently remove cells while preserving the ECM as much as possible (Wu et al., 2023). Perhaps, the incubation time of samples in DNase should be reduced to <24 h. Moreover, other detergents may improve the decellularization protocol. Previous reports have suggested that sodium deoxycholate (SDC) is better in maintaining the ECM compared to SDS (Alshaikh et al., 2020; Tiemann et al., 2020). Also, SDC perfusion has led to the creation of a 3D scaffold that closely resembles the native uterus both structurally and mechanically (Hellström et al., 2014). Perfusion of detergents through the vasculature of the whole organ is an alternative method that allows for a more controlled and uniform distribution of the decellularization solution throughout the tissue (Almeida et al., 2023). However, perfusion of small mammal organs such as those of cats and rats requires a complex protocol and advanced instruments (Padma et al., 2018). In addition, special methods such as high hydrostatic pressure should be further studied, given its

successful results in decellularizing the uterus in other species (Santoso et al., 2014). Since hydrogels generated from decellularized oviduct and uterus were reported to support the *in vitro* rabbit embryo culture system (Francés-Herrero et al., 2021; Campo et al., 2019b), it is interesting to develop this technology for application in other species including felids. There is a demand to improve the blastocyst rates of cat embryos (Hribal et al., 2014; Hui et al., 2022). Thus, our first attempt to develop a decellularization protocol for the cat oviduct and uterine horn will serve as the foundation for technologies related to improving the *in vitro* embryo culture system for felids. It is worth noting that most of the previous bioengineering research focused on decellularizing each organ separately. For instance, when an ovarian ECM scaffold was needed, only the ovary was dissected and decellularized (Pennarossa et al., 2021). To the best of the author's knowledge, this is the first study that used almost the whole reproductive tract (including ovary, oviduct, and uterine horn) in the same decellularization protocol. Given the discussion that each tissue may require its appropriate protocol (Gilbert et al., 2006), it might be advantageous to further optimize a new protocol specific to each type of tissue.

5. Conclusions

This is the first study to develop protocol for the decellularization of domestic cat's reproductive organ. When comparing the three different protocols used to decellularize the cat's reproductive tract tissues

(ovary, oviduct, and uterine horn), Protocol 3, which additionally included DNase, emerged as the method that significantly reduced DNA content and completely remove nuclear material in reproductive organs. Protocol 3 also maintained ECM content in the decellularized ovary, suggesting that this protocol can be used to further develop an ECM-derived ovarian scaffold. However, Protocol 3 reduced ECM content in oviduct and uterine horn. Here, we introduce the initial steps towards developing a decellularization process for feline reproductive organs, showcasing an effective method and biocompatible materials. The decellularization protocol established in this study is poised to become a foundational advancement for ARTs, playing a pivotal role in the conservation, clinical treatment, and experimental breeding of felid species.

CRedit authorship contribution statement

Phakjira Sanguansook: Writing – review & editing, Writing – original draft, Validation, Methodology, Investigation, Formal analysis, Data curation. **Cristina Martínez-López:** Writing – review & editing, Methodology, Investigation, Formal analysis, Data curation. **M^o. José Izquierdo-Rico:** Writing – review & editing, Validation, Supervision, Project administration, Investigation, Conceptualization. **Carlos Martínez-Cáceres:** Writing – review & editing, Validation, Software, Methodology, Investigation, Formal analysis, Data curation. **Marina López-Orozco:** Methodology, Investigation. **Kaywalee Chatdarong:** Writing – review & editing, Supervision, Investigation, Conceptualization. **Francisco Alberto García-Vázquez:** Writing – review & editing, Validation, Supervision, Project administration, Investigation, Funding acquisition, Formal analysis, Data curation, Conceptualization.

Declaration of competing interest

None

Acknowledgements

This research project is supported by Second Century Fund (C2F, Batch 1, 2019), Chulalongkorn university, PID2021-123091NB-C21 financiado por MCIN/ AEI /10.13039/501100011033/ y por FEDER Una manera de hacer Europa, and by the Ministry of Science and Innovation (PID2019-106380RB-I00/AEI/10.13039/501100011033). We would like to thank Maria Teresa Coronado Parra and Francisco Asensio Vidal for their assistance in processing samples for electron microscopy (Microscopy section, ACTI, University of Murcia). The authors also thank Prof. Paisan Tienthai for his guidance to interpret electron microscopy result.

Appendix A. Supplementary data

Supplementary data to this article can be found online at <https://doi.org/10.1016/j.rvsc.2024.105257>.

References

Alaee, S., Asadollahpour, R., Hosseinzadeh Colagar, A., Talaei-Khozani, T., 2021. The decellularized ovary as a potential scaffold for maturation of preantral ovarian follicles of prepubertal mice. *Syst Biol Reprod Med* 67, 413–427.

Almeida, G.H.D.R., da Silva-Júnior, L.N., Gibin, M.S., dos Santos, H., de Oliveira, Horvath-Pereira B., Pinho, L.B.M., et al., 2023. Perfusion and Ultrasonication produce a decellularized porcine whole-ovary scaffold with a preserved microarchitecture. *Cells* 12, 1864.

Alshaiikh, A.B., Padma, A.M., Dehlin, M., Akouri, R., Song, M.J., Brännström, M., et al., 2020. Decellularization and recellularization of the ovary for bioengineering applications; studies in the mouse. *Reprod. Biol. Endocrinol.* 18, 75.

Bruyneel, A.A.N., Carr, C.A., 2017. Ambiguity in the presentation of decellularized tissue composition: the need for standardized approaches. *Artif. Organs* 41, 778–784.

Campo, H., Baptista, P.M., López-Pérez, N., Faus, A., Cervelló, I., Simón, C., 2017. Decellularization of the pig uterus: a bioengineering pilot study. *Biol. Reprod.* 96, 34–45.

Campo, H., Cervelló, I., Pellicer, A., 2019a. Bioengineering strategies of the uterus towards improving current investigative models and female reproductive health. *Facts Views Vis. Obgyn* 11, 87–99.

Campo, H., García-Domínguez, X., López-Martínez, S., Faus, A., Vicente Antón, J.S., Marco-Jiménez, F., et al., 2019b. Tissue-specific decellularized endometrial substratum mimicking different physiological conditions influences in vitro embryo development in a rabbit model. *Acta Biomater.* 89, 126–138.

Cebotari, S., Tudorache, I., Jaekel, T., Hilfiker, A., Dorfman, S., Ternes, W., et al., 2010. Detergent decellularization of heart valves for tissue engineering: toxicological effects of residual detergents on human endothelial cells. *Artif. Organs* 34, 206–210.

Colombo, M., Alkali, L.M., Prochowska, S., Luvoni, G.C., 2021. Fighting like cats and dogs: challenges in domestic carnivore oocyte development and promises of innovative culture systems. *Animals* 11, 2135.

Comizzoli, P., Paulson, E.E., McGinnis, L.K., 2018. The mutual benefits of research in wild animal species and human-assisted reproduction. *J. Assist. Reprod. Genet.* 35, 551–560.

Crapo, P.M., Gilbert, T.W., Badylak, S.F., 2011. An overview of tissue and whole organ decellularization processes. *Biomaterials* 32, 3233–3243.

Daryabari, S.S., Kajbafzadeh, A.M., Fendereski, K., Ghorbani, F., Dehnavi, M., Rostami, M., et al., 2019. Development of an efficient perfusion-based protocol for whole-organ decellularization of the ovine uterus as a human-sized model and in vivo application of the bioscaffolds. *J. Assist. Reprod. Genet.* 36, 1211–1223.

Daryabari, S.S., Fendereski, K., Ghorbani, F., Dehnavi, M., Shafikhani, Y., Omranipour, A., et al., 2022. Whole-organ decellularization of the human uterus and in vivo application of the bio-scaffolds in animal models. *J. Assist. Reprod. Genet.* 39, 1237–1247.

Dhandapani, V., Vermette, P., 2023. Decellularized bladder as scaffold to support proliferation and functionality of insulin-secreting pancreatic cells. *J Biomed Mater Res B Appl Biomater* 111, 1890–1902.

Dietrich, G.J., Zabowska, M., Wojtczak, M., Stowińska, M., Kucharczyk, D., Ciereszko, A., 2007. Effects of different surfactants on motility and DNA integrity of brown trout (*Salmo trutta fario*) and common carp (*Cyprinus carpio*) spermatozoa. *Reprod. Biol.* 7, 127–142.

Fazelian-Dehkordi, K., Talaei-Khozani, T., A SFM., 2022. Three-dimensional in vitro maturation of rabbit oocytes enriched with sheep decellularized greater omentum. *Vet. Med. Sci.* 8, 2092–2103.

Francés-Herrero, E., De Miguel-Gómez, L., López-Martínez, S., Campo, H., García-Domínguez, X., Directo, G., et al., 2021. Development of decellularized oviductal hydrogels as a support for rabbit embryo culture. *Reprod. Sci.* 28, 1644–1658.

Francés-Herrero, E., Lopez, R., Campo, H., de Miguel-Gómez, L., Rodríguez-Eguren, A., Faus, A., et al., 2023. Advances of xenogeneic ovarian extracellular matrix hydrogels for in vitro follicle development and oocyte maturation. *Biomater Adv.* 151, 213480.

Gilbert, T.W., Sellaro, T.L., Badylak, S.F., 2006. Decellularization of tissues and organs. *Biomaterials* 27, 3675–3683.

Grauss, R.W., Hazekamp, M.G., van Vliet, S., Gittenberger-de Groot, A.C., DeRuiter, M. C., 2003. Decellularization of rat aortic valve allografts reduces leaflet destruction and extracellular matrix remodeling. *J. Thorac. Cardiovasc. Surg.* 126, 2003–2010.

Hassanpour, A., Talaei-Khozani, T., Kargar-Abarghouei, E., Razban, V., Vojdani, Z., 2018. Decellularized human ovarian scaffold based on a sodium lauryl ester sulfate (SLES)-treated protocol, as a natural three-dimensional scaffold for construction of bioengineered ovaries. *Stem Cell Res Ther* 9, 252.

Hellström, M., El-Akouri, R.R., Sihlbom, C., Olsson, B.M., Lengqvist, J., Bäckdahl, H., et al., 2014. Towards the development of a bioengineered uterus: comparison of different protocols for rat uterus decellularization. *Acta Biomater.* 10, 5034–5042.

Hoenig, M., 2012. The cat as a model for human obesity and diabetes. *J. Diabetes Sci. Technol.* 6, 525–533.

Hrebikova, H., Diaz, D., Mokry, J., 2015. Chemical decellularization: a promising approach for preparation of extracellular matrix. *Biomed. Pap. Med. Fac. Univ. Palacky Olomouc Czech Repub.* 159, 12–17.

Hribal, R., Hachen, A., Jewgenow, K., Zahmel, J., Fernandez-Gonzalez, L., Braun, B.C., 2014. The influence of recombinant feline oviductin on different aspects of domestic cat (*Felis catus*) IVF and embryo quality. *Theriogenology* 82, 742–749.

Hui, L., Ning, W., Rongjing, Y., Shen, Y., Bao, Y., Jian, C., et al., 2022. First deliveries of felines by transcervical transfer of in vitro-cultured embryos. *Theriogenology* 193, 30–36.

Jewgenow, K., Paris, M.C.J., 2006. Preservation of female germ cells from ovaries of cat species. *Theriogenology* 66, 93–100.

Jewgenow, K., Braun, B.C., Dehnhard, M., Zahmel, J., Goeritz, F., 2017. Research on reproduction is essential for captive breeding of endangered carnivore species. *Reprod. Domest. Anim.* 52 (Suppl. 2), 18–23.

Kim, S.W., Kim, Y.Y., Kim, H., Ku, S.Y., 2021. Recent advancements in engineered biomaterials for the regeneration of female reproductive organs. *Reprod. Sci.* 28, 1612–1625.

López-Martínez, S., Rodríguez-Eguren, A., de Miguel-Gómez, L., Francés-Herrero, E., Faus, A., Díaz, A., et al., 2021. Bioengineered endometrial hydrogels with growth factors promote tissue regeneration and restore fertility in murine models. *Acta Biomater.* 135, 113–125.

Masoomikarimi, M., Salehi, M., Noorbakhsh, F., Rajaei, S., 2023. A combination of physical and chemical treatments is more effective in the preparation of acellular uterine scaffolds. *Cell J.* 25, 25–34.

McIntyre, R.L., Levy, J.K., Roberts, J.F., Reep, R.L., 2010. Developmental uterine anomalies in cats and dogs undergoing elective ovariectomy. *J. Am. Vet. Med. Assoc.* 237, 542–546.

Mirzaeian, L., Eivazkhani, F., Hezavehei, M., Moini, A., Esfandiari, F., Valojerdi, M.R., et al., 2020. Optimizing the cell seeding protocol to human decellularized ovarian scaffold: application of dynamic system for bio-engineering. *Cell J.* 22, 227–235.

- Neishabouri, A., Soltani Khaboushan, A., Daghigh, F., Kajbafzadeh, A.-M., Majidi, Zolbin M., 2022. Decellularization in tissue engineering and regenerative medicine: evaluation, modification, and application methods. *Front. Bioeng. Biotechnol.* 10.
- Nikniaz, H., Zandieh, Z., Nouri, M., Daei-Farshbaf, N., Aflatoonian, R., Gholipourmalekabadi, M., et al., 2021. Comparing various protocols of human and bovine ovarian tissue decellularization to prepare extracellular matrix-alginate scaffold for better follicle development in vitro. *BMC Biotechnol.* 21, 8.
- Padma, A.M., Tiemann, T.T., Alshaikh, A.B., Akouri, R., Song, M.J., Hellström, M., 2018. Protocols for rat uterus isolation and decellularization: applications for uterus tissue engineering and 3D cell culturing. *Methods Mol. Biol.* 1577, 161–175.
- Padma, A.M., Alshaikh, A.B., Song, M.J., Akouri, R., Oltean, M., Brännström, M., et al., 2021. Decellularization protocol-dependent damage-associated molecular patterns in rat uterus scaffolds differentially affect the immune response after transplantation. *J. Tissue Eng. Regen. Med.* 15, 674–685.
- Park, E.Y., Park, J.H., Mai, N.T.Q., Moon, B.S., Choi, J.K., 2023. Control of the growth and development of murine preantral follicles in a biomimetic ovary using a decellularized porcine scaffold. *Mater Today Bio.* 23, 100824.
- Pelican, K.M., Wildt, D.E., Pukazhenthil, B., Howard, J., 2006. Ovarian control for assisted reproduction in the domestic cat and wild felids. *Theriogenology* 66, 37–48.
- Pennarossa, G., Ghiringhelli, M., Gandolfi, F., Brevini, T.A.L., 2020. Whole-ovary decellularization generates an effective 3D bioscaffold for ovarian bioengineering. *J. Assist. Reprod. Genet.* 37, 1329–1339.
- Pennarossa, G., De Iorio, T., Gandolfi, F., Brevini, T.A.L., 2021. Ovarian Decellularized bioscaffolds provide an optimal microenvironment for cell growth and differentiation in vitro. *Cells* 10.
- Pope, C.E., McRae, M.A., Plair, B.L., Keller, G.L., Dresser, B.L., 1997. In vitro and in vivo development of embryos produced by in vitro maturation and in vitro fertilization of cat oocytes. *J. Reprod. Fertil. Suppl.* 51, 69–82.
- Pope, C.E., Gómez, M.C., Dresser, B.L., 2006. In vitro production and transfer of cat embryos in the 21st century. *Theriogenology* 66, 59–71.
- Pors, S.E., Ramløse, M., Nikiforov, D., Lundsgaard, K., Cheng, J., Andersen, C.Y., et al., 2019. Initial steps in reconstruction of the human ovary: survival of pre-antral stage follicles in a decellularized human ovarian scaffold. *Hum. Reprod.* 34, 1523–1535.
- Prochowska, S., Nizański, W., Snoeck, F., Wydooghe, E., Van Soom, A., Kochan, J., et al., 2022. How can we introduce ART into wild felid conservation in practice? Joint experience in semen collection from captive wild felids in Europe. *Animals* 12, 871.
- Santoso, E.G., Yoshida, K., Hirota, Y., Aizawa, M., Yoshino, O., Kishida, A., et al., 2014. Application of detergents or high hydrostatic pressure as decellularization processes in uterine tissues and their subsequent effects on in vivo uterine regeneration in murine models. *PLoS One* 9, e103201.
- Songsasen, N., Comizzoli, P., Nagashima, J., Fujihara, M., Wildt, D.E., 2012. The domestic dog and cat as models for understanding the regulation of ovarian follicle development in vitro. *Reprod. Domest. Anim.* 47 (Suppl. 6), 13–18.
- Thongphakdee, A., Sukparangsi, W., Comizzoli, P., Chatdarong, K., 2020. Reproductive biology and biotechnologies in wild felids. *Theriogenology* 150, 360–373.
- Tiemann, T.T., Padma, A.M., Sehic, E., Bäckdahl, H., Oltean, M., Song, M.J., et al., 2020. Towards uterus tissue engineering: a comparative study of sheep uterus decellularisation. *Mol. Hum. Reprod.* 26, 167–178.
- Tipkantha, W., Thuwanut, P., Morrell, J., Comizzoli, P., Chatdarong, K., 2016. Influence of living status (single vs. paired) and centrifugation with colloids on the sperm morphology and functionality in the clouded leopard (*Neofelis nebulosa*). *Theriogenology* 86, 2202–2209.
- Wildt, D.E., Comizzoli, P., Pukazhenthil, B., Songsasen, N., 2010. Lessons from biodiversity—the value of nontraditional species to advance reproductive science, conservation, and human health. *Mol. Reprod. Dev.* 77, 397–409.
- Woodruff, T.K., Shea, L.D., 2007. The role of the extracellular matrix in ovarian follicle development. *Reprod. Sci.* 14, 6–10.
- Wu T, Huang K-C, Yan J-F, Zhang J-J, Wang S-X. Extracellular matrix-derived scaffolds in constructing artificial ovaries for ovarian failure: a systematic methodological review. *Human Reprod. Open.* 2023;2023.
- Zahmel, J., Skalborg Simonsen, K., Stagegaard, J., Palma-Vera, S.E., Jewgenow, K., 2022. Current state of in vitro embryo production in African lion (*Panthera leo*). *Animals (Basel)* 12.
- Zhang, Y., Zhang, C., Li, Y., Zhou, L., Dan, N., Min, J., et al., 2023. Evolution of biomimetic ECM scaffolds from decellularized tissue matrix for tissue engineering: A comprehensive review. *Int. J. Biol. Macromol.* 246, 125672.